Activation of Arp2/3 by WASp Is Essential for the Endocytosis of Delta Only during Cytokinesis in *Drosophila*

Graphical Abstract
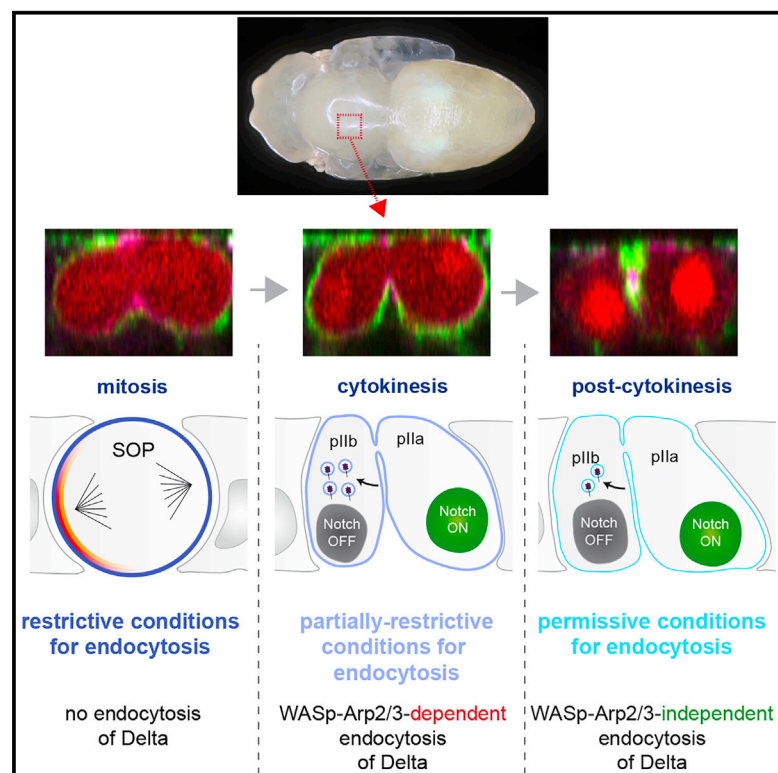
Authors

Mateusz Trylinski, François Schweisguth

Correspondence

fschweis@pasteur.fr

In Brief

WASp-Arp2/3 is required for Notch-mediated intra-lineage fate decisions. Trylinski and Schweisguth report that WASp-Arp2/3 is key for the efficient endocytosis of Delta only during cytokinesis. This helps explain how and why how actin polymerization is key for Notch activation only in the context of asymmetric cell divisions.

Highlights

- WASp-Arp2/3, but not SCAR, is required for Notch activation at cytokinesis

- SCAR, but not WASp, regulates contact expansion between SOP daughters

- WASp-Arp2/3 is required for efficient Delta endocytosis only during cytokinesis

- A pushing force generated by Arp2/3 may be needed at cytokinesis for Notch activation

CellPress

Report

Activation of Arp2/3 by WASp Is Essential for the Endocytosis of Delta Only during Cytokinesis in *Drosophila*

Mateusz Trylinski[1,2] and François Schweisguth[1,3,*]
[1]Institut Pasteur, UMR3738, CNRS, Paris 75015, France
[2]Sorbonne Université, Collège Doctoral, Paris 75005, France
[3]Lead Contact
*Correspondence: fschweis@pasteur.fr
https://doi.org/10.1016/j.celrep.2019.06.012

SUMMARY

The actin nucleator Arp2/3 generates pushing forces in response to signals integrated by SCAR and WASp. In *Drosophila*, the activation of Arp2/3 by WASp is specifically required for Notch signaling following asymmetric cell division. How WASp and Arp2/3 regulate Notch activity and why receptor activation requires WASp and Arp2/3 only in the context of intra-lineage fate decisions are unclear. Here, we find that WASp, but not SCAR, is required for Notch activation soon after division of the sensory organ precursor cell. Conversely, SCAR, but not WASp, is required to expand the cell-cell contact between the two SOP daughters. Thus, these two activities of Arp2/3 can be uncoupled. Using a time-resolved endocytosis assay, we show that WASp and Arp2/3 are required for the endocytosis of Dl only during cytokinesis. We propose that WASp-Arp2/3 provides an extra pushing force that is specifically required for the efficient endocytosis of Dl during cytokinesis.

INTRODUCTION

In animal cells, a thin cortex of actin filaments is dynamically regulated to produce the force required for basic cellular processes, such as motility, cytokinesis, and endocytosis (Pollard and Borisy, 2003). This regulation involves the nucleation of branched actin filaments by the actin-related proteins 2/3 (Arp2/3) complex (Goley and Welch, 2006; Pollard, 2007; Rotty et al., 2013). By itself, Arp2/3 is weakly active, and nucleation-promoting factors (NPFs) are needed to stimulate its nucleation activity. Thus, when and where actin-based pushing forces are produced in the cell depends on the localization and activity of the NPFs. Wiskott-Aldrich syndrome protein (WASP) family proteins are the best-studied NPFs. These are usually maintained in an autoinhibited state and can be activated at the membrane by small GTPases (Alekhina et al., 2017; Campellone and Welch, 2010; Kim et al., 2000; Mullins and Pollard, 1999; Rohatgi et al., 1999; Rotty et al., 2013). Three WASP family members are known in *Drosophila*: WASp, SCAR/WAVE (suppressor of cyclic AMP repressor/WASp-family verpolin-homologous protein),

and WASH (WASp and SCAR homolog) (Ben-Yaacov et al., 2001; Verboon et al., 2018; Zallen et al., 2002). Genetic analysis indicates that SCAR is the primary NPF in *Drosophila*, since the loss of *SCAR* activity leads to developmental and cellular defects that are similar to those seen upon the disruption of *Arp2/3* activity (Zallen et al., 2002), whereas WASH has a non-essential function during oogenesis (Nagel et al., 2017; Verboon et al., 2018), and WASp is only required for specific Notch-mediated fate decisions following asymmetric cell divisions in muscle, brain, and sensory organ lineages (Ben-Yaacov et al., 2001). This function of WASp is mediated by Arp2/3, since the loss of the Arp3 and Arpc1 subunits of the Arp2/3 complex leads to *WASp*-like cell fate defects (Rajan et al., 2009). How WASp and Arp2/3 regulate Notch signaling is unclear. In addition, given the ubiquitous expression of WASp (Rodriguez-Mesa et al., 2012) and the functional pleiotropy of Notch, it is unclear why WASp is only required for Notch signaling in the context of asymmetric cell division.

Notch receptor activation requires a pulling force to expose an otherwise buried cleavage site in the extracellular domain of Notch, the cleavage of which eventually produces the Notch intracellular domain (NICD) (Kopan and Ilagan, 2009). Previous studies have shown that endocytosis of the Notch ligands provides a strong enough pulling force to direct receptor activation (Henrique and Schweisguth, 2019; Langridge and Struhl, 2017; Lovendahl et al., 2018). Since WASp and Arp2/3 are known to increase the efficiency of endocytosis by nucleating branched filaments shortly after membrane ingression begins (i.e., when high forces are required) (Kaksonen and Roux, 2018; Mund et al., 2018; Picco et al., 2018), it is conceivable that WASp-stimulated Arp2/3 activity may facilitate receptor activation by regulating the endocytosis of the Notch ligand Delta (Dl). However, it was reported that the endocytosis did not depend on Arp3 (Rajan et al., 2009), clearly arguing against this model. It was proposed that Arp2/3 may instead regulate the transport of endocytosed Dl back to the apical membrane, where it would activate Notch (Rajan et al., 2009). This model, however, is not supported by a recent photo-tracking analysis of fluorescent Notch receptors, showing that signaling takes place along the lateral membrane following asymmetric division. NICD was produced during cytokinesis from a subset of Notch receptors that are located basal to the midbody (Trylinski et al., 2017). Thus, how WASp-Arp2/3 positively regulates Notch signaling is not known.

Sensory organ precursor (SOP) cells provide an excellent model to address how WASp regulates Notch. SOP cells divide
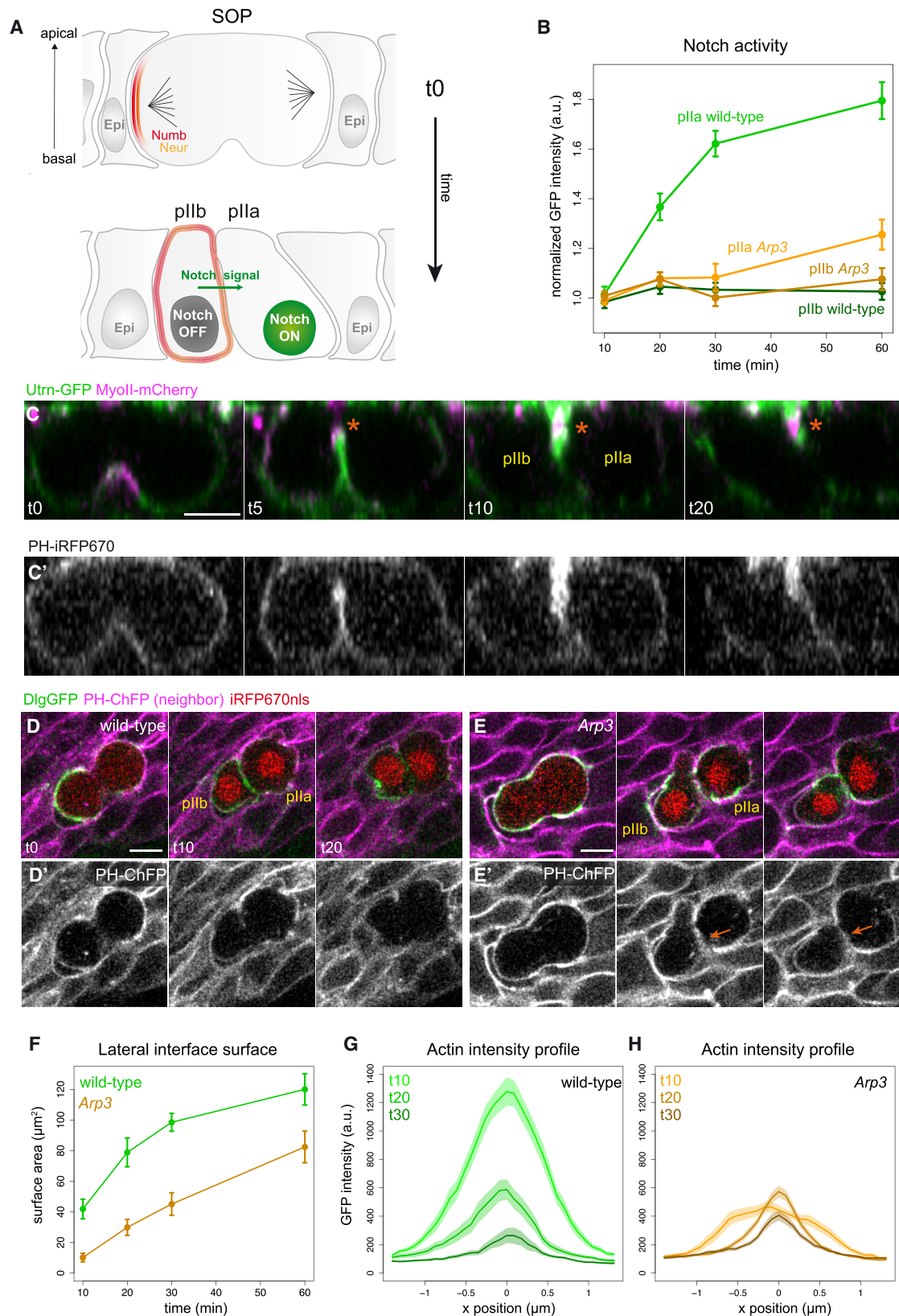
(legend on next page)

asymmetrically in the pupal notum to produce a posterior pIIa and an anterior pIIb. The binary pIIa-pIIb decision is regulated by Notch, WASp, and Arp2/3 (Figure 1A; Ben-Yaacov et al., 2001; Rajan et al., 2009; Schweisguth, 2015). Asymmetry in Notch activity results from the unequal segregation of Neuralized (Neur), an E3 ubiquitin ligase targeting Dl (Le Borgne and Schweisguth, 2003), and Numb, a recycling inhibitor of Notch (Cotton et al., 2013; Couturier et al., 2012, 2013, 2014; Johnson et al., 2016; Rhyu et al., 1994). Here, we used live imaging to show that WASp and Arp2/3 are required for receptor activation at the time of cytokinesis. This early loss of Notch signaling in *WASp* and *Arp3* mutants did not merely result from a defect in pIIa-pIIb contact expansion at cytokinesis. Contact expansion involves the activation of Arp2/3 by Rac and SCAR, but not by WASp, and SCAR and Rac are dispensable for Notch activation during cytokinesis and pIIa specification. Thus, Arp2/3 has separable functions in contact expansion and Notch signaling at cytokinesis. Instead, our detailed analysis of the endocytosis of Dl revealed that WASp is required for the efficient endocytosis of Dl during cytokinesis, but not afterward. This specific requirement of WASp and Arp2/3 for endocytosis during cytokinesis only may explain its specific requirement in Notch-mediated intra-lineage decision.

RESULTS

Arp3 Is Required for Notch Signaling and Contact Expansion during Cytokinesis

While the Arp2/3 complex is essential for the pIIa-pIIb decision (Rajan et al., 2009), when and how the loss of Arp2/3 activity affects Notch activity is not known. To monitor signaling dynamics, we used a GFP-tagged Notch receptor and measured the level of nuclear GFP fluorescence as a proxy for NICD (Trylinski et al., 2017). As previously shown (Couturier et al., 2012; Trylinski et al., 2017), Notch is activated in pIIa cells at cytokinesis, between t10 and t30 (time [t] is in minutes; t0 corresponds to the metaphase-anaphase transition). Conversely, NICD did not accumulate in pIIb nuclei (Figures 1B, S1A, and S1B). In contrast, an early and strong reduction of NICD was observed in *Arp3* mutant pIIa, and low NICD levels were detected at t60

(Figure 1B). In addition, Notch accumulated into dots along the pIIa-pIIb interface in *Arp3* mutant clones (Figure S1B), as in *Presenilin* mutants (Trylinski et al., 2017), which is suggestive of reduced Notch cleavage. We conclude that the activity of Arp2/3 is required for Notch receptor activation during cytokinesis (i.e., earlier than the Dl trafficking defects seen in *Arp3* mutant cells) (Rajan et al., 2009).

In dividing epidermal cells, Arp2/3 regulates actin polymerization to produce a force pushing the plasma membrane of the two sister cells, one against the other. This promotes cell-cell contact and excludes neighboring epidermal cells from this interface (Herszterg et al., 2013). Here, we extend these observations to dividing SOP cells using utrophin-GFP (Utrn-GFP; utrophin actin-binding domain fused to GFP) to image F-actin dynamics. A transient accumulation of cortical F-actin formed basal to the midbody and progressively expanded (Figures 1C, 1C′, and S2A; quantification in Figure 1G). A GFP-tagged Arp3 showed a similar distribution (Figures S1E and S1E′), and F-actin was strongly reduced in *Arp3* mutants (Figures 1H and S2B), indicating that Arp2/3 regulates actin polymerization along the lateral pIIa-pIIb contact. We next studied the expansion of the lateral pIIa-pIIb contact using a genetic mosaic assay whereby the plasma membrane of the neighboring epidermal cells was specifically labeled such that its withdrawal from the pIIa-pIIb contact could be easily followed (Herszterg et al., 2013). Wild-type and *Arp3* mutant SOP cells that were surrounded by epidermal cells expressing a membrane marker (pleckstrin homology (PH)-mCherry fluorescent protein, PH-ChFP) were selected for analysis. In wild-type clones, the pIIa-pIIb cells rapidly formed a long cell-cell contact, as revealed by the rapid withdrawal of the labeled membranes of neighboring epidermal cells from this contact area (Figures 1D and 1D′; Video S1). In contrast, in *Arp3* mutant clones, sister cells exhibited reduced contact for a longer period of time (Figures 1E and 1E′; Video S1). This resulted in a smaller lateral contact area at t10–t30 (i.e., when Notch signaling normally occurs) (Figure 1F). Of note, our observation that *Arp3* mutant cells surrounded by wild-type epidermal cells exhibited cytokinesis defects (Figures 1E and 1E′) implies that Arp2/3 acts in a lineage-autonomous manner for the expansion of the pIIa-pIIb contact. Similarly,

Figure 1. *Arp3* Is Required for Notch Activation and Contact Expansion
(A) Asymmetric division of an SOP within the notum epithelium (Epi, epidermal cell; t0, anaphase). Numb (red) and Neur (orange) localize at the anterior cortex (top), leading to fate asymmetry (bottom). Notch is inhibited in pIIb and activated in pIIa (bottom). In this article, t0 corresponds to the metaphase-anaphase transition. Anterior is to the left.
(B) Time course accumulation of nuclear NiGFP in wild-type and *Arp3* pIIa and pIIb cells. NICD rapidly accumulated after division in wild-type pIIa. In contrast, low NICD levels were detected only at t60 in *Arp3* pIIa cells. Means ± SEMs are shown in this and all of the other graphs; n ≥ 20 cells for each time point, 7 pupae.
(C and C′) Snapshots showing the dynamic distribution of F-actin (C; Utrn-GFP, green), myosin (C; MyoII-Cherry, magenta) in a dividing SOP marked by PH-iRFP670, a membrane marker that binds phosphatidylinositol 4,5-biphosphaste (PIP2; C′). The membrane ingresses from the basal side (apical midbody marked by MyoII, *). F-actin and PIP2 transiently accumulated along the lateral pIIa-pIIb contact from t5 to t20. Apical is up. In this and all other panels, anterior is to the left.
(D–E′) Live imaging analysis of contact expansion in wild-type (D and D′) and *Arp3* dividing SOPs (E and E′; Video S1). All of the cells expressed GFP-tagged Discs-large (DlgGFP, green; best detected in dividing cells in these z sections), whereas SOP cells were marked by a nuclear infrared fluorescent protein (iRFP670nls, red). PH-ChFP− SOP cells surrounded by PH-ChFP+ epidermal cells were selected for analysis. The membranes of the neighboring wild-type epidermal cells were not efficiently withdrawn from the new cell-cell contact formed by *Arp3* mutant pIIa-pIIb cells (arrow in E′; compare with wild-type, D′).
(F) Time course analysis of the lateral contact area in wild-type (n = 14 cells, 6 pupae) and *Arp3* (n = 15 cells, 6 pupae) pIIa-pIIb pairs. A delay in lateral contact expansion was seen upon the loss of *Arp3* activity.
(G and H) F-actin intensity profiles in wild-type (G) and *Arp3* (H) pIIa-pIIb pairs at t10, t20, and t30. F-actin levels were measured using Utrn-GFP. *Arp3* was required for F-actin accumulation along the lateral pIIa-pIIb interface during cytokinesis (n = 18 cells, 4 pupae for wild-type; n = 22 cells, 4 pupae for *Arp3*).
In these and all other figures, except Figure S4, scale bars represent 5 μm. See also Figure S1 and Video S1.
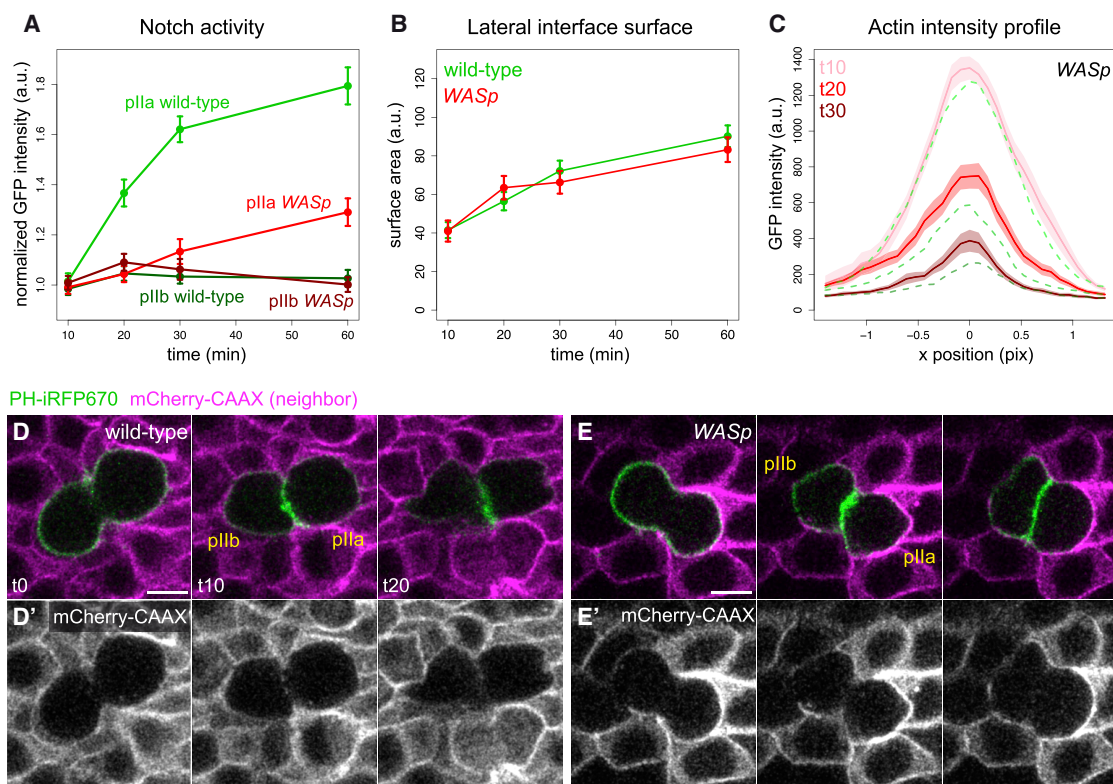
Figure 2. WASp Is Required for Notch Activation, but Not for Contact Expansion

(A) Time course analysis of NICD accumulation in *WASp* mutant cells (wild-type data are from Figure 1B). Low Notch activity could only be detected at t60 in pIIa, showing that *WASp* is required for the activation of Notch. n ≥ 20 cells for each time point, 5 pupae.

(B and C) Lateral contact area (B; *WASp*: n = 8 cells, 1 pupa; wild-type: n = 15 cells, 3 pupae) and F-actin intensity profiles (C; *WASp*: n = 21 cells, 3 pupae; wild-type mean values from Figure 1G are shown with green dashed lines). The loss of *WASp* did not affect the pIIa-pIIb contact or the F-actin dynamics during cytokinesis.

(D–E′) Snapshots of wild-type (D and D′) and *WASp* mutant (E and E′) pupae in which SOP cells were marked by PH-iRFP670 (green) and epidermal cells expressed mCherry-CAAX (magenta). Cell-cell contact was rapidly established between pIIa and pIIb in both wild-type and *WASp* mutants, as seen by the withdrawal of the plasma membrane of the neighboring epidermal cells.

See also Figures S1 and S2 and Video S2.

analysis of NICD levels in *Arp3* mutant clones showed that the activity of Arp2/3 is also required within the pIIa-pIIb cell pair for Notch activation (Figures S1F and S1G′′).

In summary, our data indicate that Arp2/3 regulates the rapid expansion of the pIIa-pIIb contact via the formation of a cortical F-actin wave during cytokinesis and is also required for Notch receptor activation at this precise stage.

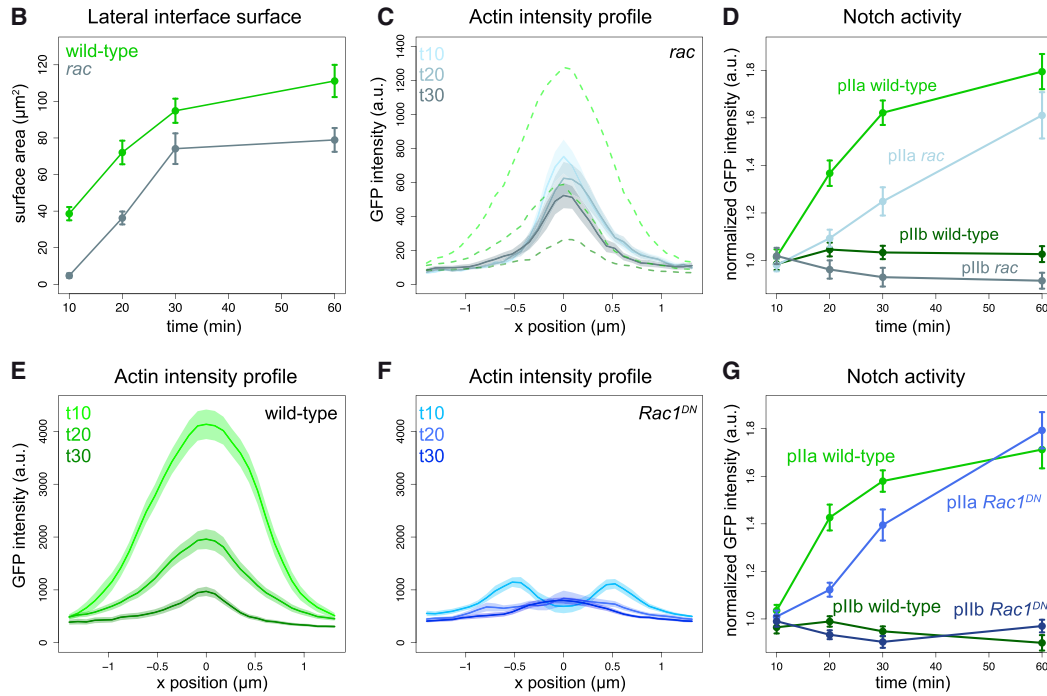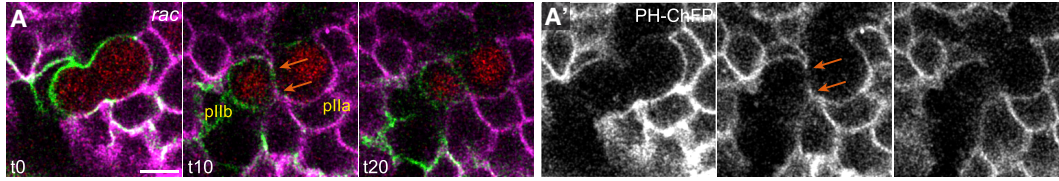### WASp Is Required for Notch Signaling, but Not for pIIa-pIIb Contact Expansion

Given that Notch receptor activation is contact dependent and that signaling strength may vary with the cell-cell contact area (Guisoni et al., 2017; Shaya et al., 2017), we wondered whether the loss of Arp2/3 may cause a loss of Notch activation through its role in regulating cell-cell contact. To address this, we re-examined the role of WASp in SOP cells using live imaging. As in *Arp3* mutant cells, a strong decrease in NICD accumulation was measured in *WASp* mutant pIIa cells at cytokinesis (Figure 2A) and Notch accumulated along the lateral pIIa-pIIb interface (Figure S1C). These data confirmed that WASp acts as an

Arp2/3 NPF for Notch signaling (Tal et al., 2002). Next, we studied cytokinesis in *WASp* mutant pupae using a membrane-bound ChFP that was specifically expressed in epidermal cells (*pnr^ts > mCherry-CAAX* combined with *neur-Gal80*; see Method Details). We found that the loss of *WASp* activity had no significant effect on contact expansion (Figures 2B, 2D, and 2E′; Video S2) or F-actin accumulation along the pIIa-pIIb interface (Figures 2C and S2C). We therefore conclude that the activation of Arp2/3 by WASp is only required for Notch signaling during cytokinesis but is dispensable for both transient cortical actin wave and expansion of the pIIa-pIIb contact. Since these two activities of Arp2/3 can be uncoupled, we can rule out the possibility that the Notch signaling defect seen in *Arp3* mutants merely results from a cell-cell contact defect.

Rac and SCAR/WAVE Are Required for pIIa-pIIb Contact Expansion

Our *WASp* mutant analysis suggests that another NPF regulates Arp2/3 to promote contact expansion at cytokinesis. In epidermal cells, the Arp2/3-dependent actin wave depends on

DlgGFP PH-ChFP (neighbor) iRFP670nls

A *rac*
t0   pIIb pIIa t10   t20

A' PH-ChFP

B Lateral interface surface

wild-type
rac

C Actin intensity profile
t10
t20
t30
rac

D Notch activity
pIIa wild-type
pIIa *rac*
pIIb wild-type
pIIb *rac*

E Actin intensity profile
t10
t20
t30
wild-type

F Actin intensity profile
t10
t20
t30
Rac1^{DN}

G Notch activity
pIIa wild-type
pIIa *Rac1^{DN}*
pIIb wild-type
pIIb *Rac1^{DN}*

PH-ChFP Resille-GFP (neighbor) iRFP670nls

H wild-type
t0   pIIb pIIa t10   t20

I *SCAR*
pIIb pIIa

H' Resille-GFP

I' Resille-GFP

J Lateral interface surface
wild-type
SCAR

K Actin intensity profile
t10
t20
t30
SCAR

L Notch activity
pIIa wild-type
pIIa *SCAR*
pIIb wild-type
pIIb *SCAR*
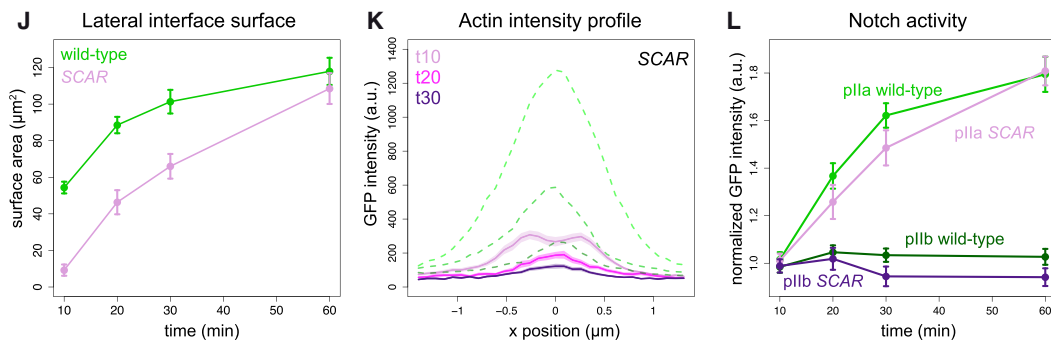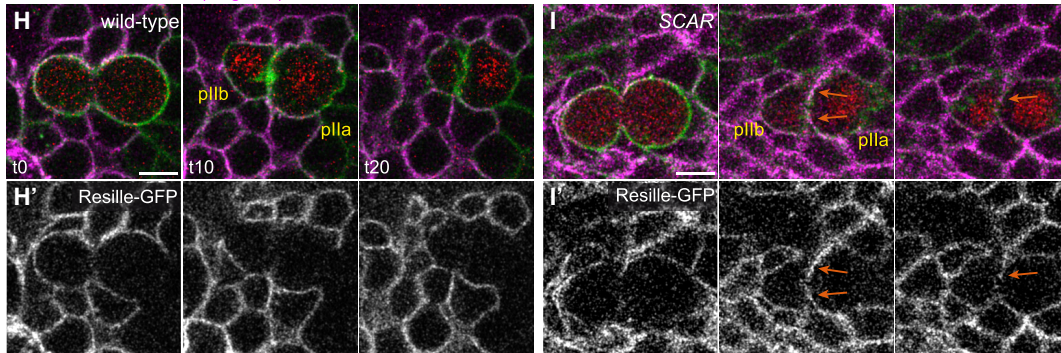
(legend on next page)

Rac (Herszterg et al., 2013) acting upstream of SCAR/WAVE to activate Arp2/3 (Eden et al., 2002; Yamada and Nelson, 2007). Three *Rac* family genes are encoded by the fly genome: *Rac1*, *Rac2*, and *Mig-2-like* (*Mtl*) (Hakeda-Suzuki et al., 2002). To test the role of Rac activity in pIIa-pIIb contact expansion, we performed live imaging in clones of cells that are double mutant for *Rac1* and *Rac2* and heterozygous for *Mtl*. Live imaging of these mutant cells, called *rac*, indicated that both contact expansion and F-actin accumulation at the pIIa-pIIb interface were significantly affected (Figures 3A–3C and S2D; Video S1), albeit to a slightly lesser extent than in *Arp3* mutant clones (see Figures 1F and 1H; this difference may result from the remaining Rac activity produced by one copy of the *Mtl* gene or from partial redundancy with other NPFs). Furthermore, the expression of a dominant-negative form of Rac1 (Rac1^{N17}, called Rac1^{DN}) led to a strong reduction in F-actin at cytokinesis (Figures 3E, 3F, S3B, and S3B′; Video S3) and pIIa-pIIb contact defects at t10–t30 (Figures S3B–S3D). Finally, GFP-tagged Rac1 localized along the lateral pIIa-pIIb interface at cytokinesis (Figures S3A and S3A′). These results suggest that Rac regulates contact expansion through the regulation of the Arp2/3-dependent wave of cortical F-actin. However, despite these defects in cell-cell contact, relatively high NICD levels were measured in *rac* and *Rac1^{DN}* pIIa cells at t10–t30 and NICD accumulated to levels similar to wild-type levels at t60 (Figures 3D and 3G). We suggest that the delay in NICD accumulation seen in *rac* and *Rac1^{DN}* pIIa may result from the delay in contact expansion. Thus, Rac primarily regulates contact expansion, presumably via Arp2/3, but not Notch receptor activation.

One of the main effector of Rac GTPases for Arp2/3-mediated contact expansion is SCAR/WAVE (Alekhina et al., 2017; Del Signore et al., 2018). To test whether SCAR, like Rac, regulates contact expansion but not Notch signaling, we next studied *SCAR* mutant clones. Consistent with Rac regulating SCAR-mediated activation of Arp2/3, both F-actin accumulation and

lateral contact expansion at the pIIa-pIIb interface were strongly impaired (Figures 3H–3K and S2E; Video S4). In contrast, the accumulation of NICD in pIIa was barely affected (Figure 3L). We conclude that the activation of Arp2/3 by SCAR is required for the transient cortical actin wave and for the contact expansion between pIIa and pIIb, but not for Notch signaling at cytokinesis. In summary, Rac-SCAR, but not WASp, activates the Arp2/3 complex at cytokinesis to promote the rapid formation of the pIIa-pIIb contact, whereas WASp, but not Rac-SCAR, is required for strong Notch activation at cytokinesis.

Activation of Arp2/3 by WASp Is Required for the Efficient Endocytosis of Dl at Cytokinesis Only

We next addressed how WASp-Arp2/3 regulates Notch signaling. A previous study suggested that the endocytosis of Dl in SOP progeny cells does not depend on Arp2/3, but reported a trafficking defect for endocytosed Dl 60 min after internalization (Rajan et al., 2009). Because this defect was observed 40 min after a loss of Notch activity was observed (Figure 1B), the mis-trafficking of Dl is unlikely to cause the loss of Notch activity. Given the general role of WASp in endocytosis (Kaksonen and Roux, 2018; Mund et al., 2018; Picco et al., 2018) and the role of Dl endocytosis in pIIb for receptor activation in pIIa (Le Borgne and Schweisguth, 2003), we decided to re-investigate the possible role of WASp and Arp2/3 in the endocytosis of Dl. We first examined the distribution of a functional GFP-tagged Dl, DlGFP (Corson et al., 2017), using live imaging. In wild-type cells, DlGFP was hardly detected at the pIIa-pIIb interface using direct fluorescence (Figure 4A) due to its rapid turnover (Trylinski et al., 2017). In contrast, DlGFP was detected in dots at the pIIa-pIIb lateral cortex in *Arp3* and *WASp* mutant cells at t20 (Figures 4B and 4C). This suggests that Dl has a slower turnover in these mutants, possibly due to reduced endocytosis. To test this, we quantified the GFP fluorescence signal of DlGFP in the pIIb

---

Figure 3. Rac and SCAR Are Required for Contact Expansion, but Not for Notch Activity

(A and A′) Snapshots of *rac* mutant cells, marked by the loss of PH-ChFP (magenta in A), showing that cell-cell contact was not yet established at t10 between pIIa and pIIb (arrows; A, 3-color snapshot with iRFPnls marking the dividing SOP; A′, PH-ChFP channel only): the plasma membrane of the neighboring epidermal cells was withdrawn only at t20 (compare with Figures 1D and 1D′).

(B and C) Lateral contact area (B; n = 10 cells and n = 3 pupae) and F-actin intensity (C; n = 11 cells, 2 pupae; wild-type mean values from Figure 1G, green dashed lines) profiles in *rac* mutant cells. The activity of *rac* is required for the rapid withdrawal of neighboring membranes and for F-actin polymerization during cytokinesis.

(D) Time course analysis of NICD accumulation in *rac* mutant cells (wild-type data are from Figure 1B). A delay in Notch signaling was observed. n ≥ 14 cells for each time point, 4 pupae.

(E and F) F-actin intensity profiles in wild-type (E; n = 24 cells, 3 pupae) and Rac1^{DN} expressing cells (F; n = 26 cells, 3 pupae), as determined using LifeAct-GFP expressed in SOP cells under the control of *neurPGal4 Gal80^{ts}* at 29°C (from 0 h after puparium formation [APF]). Rac1^{DN} strongly reduced F-actin accumulation at the pIIa-pIIb interface during cytokinesis.

(G) Time course analysis of NICD accumulation in Rac1^{DN}-expressing cells (n = 20 cells for each time point, 5 pupae). Rac1^{DN} was expressed in SOPs using *neurPGal4 Gal80^{ts}* (29°C from 0 h APF; wild-type controls are *NiGFP neurPGal4 Gal80^{ts}* transferred to 29°C at 0 h APF; n = 17 cells for each time point, 4 pupae). A slight delay in nuclear NiGFP accumulation was observed in pIIa upon expression of Rac1^{DN}.

(H–I′) Live imaging of contact expansion in wild-type (H and H′) and *SCAR* mutant (I and I′) SOP cells (iRFPnls, red). Contact expansion was studied in SOP cells that had lost the Resille-GFP marker (magenta) and that were surrounded by wild-type cells expressing this marker. All of the cells expressed PH-ChFP (green). The membrane of the neighboring epidermal cells was withdrawn at ~t10 from wild-type pIIa-pIIb pairs, but only at ~t20 in *SCAR* mutants.

(J) Time course analysis of the lateral contact area in wild-type (n = 12 cells, 3 pupae) and *SCAR* pIIa-pIIb pairs (n = 10 cells, 3 pupae) using the markers shown in (H)–(I′). A delay in lateral contact expansion was seen upon the loss of *SCAR* activity.

(K) F-actin intensity profiles in *SCAR* mutant cells, as determined using Utrn-GFP (n = 18 cells, 3 pupae; wild-type mean values from Figure 1G, green dashed lines). F-actin failed to accumulate at the pIIa-pIIb contact during cytokinesis.

(L) Nuclear NiGFP levels in *SCAR* mutant cells (n = 21 cells, 5 pupae; wild-type data from Figure 1B). The loss of *SCAR* activity did not significantly affect the Notch signaling dynamics.

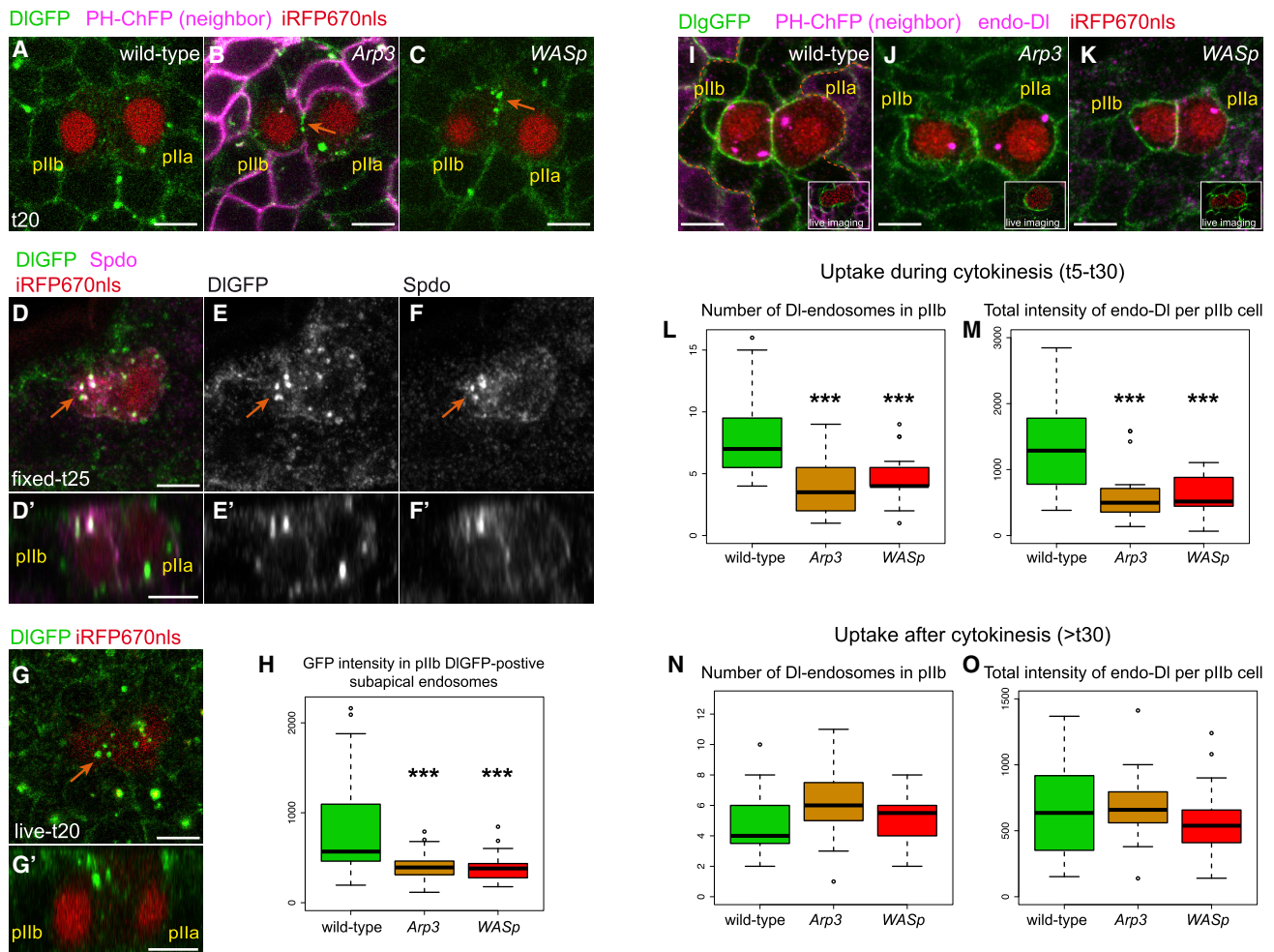See also Figures S2 and S3 and Videos S1, S3, and S4.

Figure 4. Arp2/3 and WASp Are Required for the Endocytosis of Dl Only during Cytokinesis

(A–C) Localization of DlGFP (green) in wild-type (A), *Arp3* (B), and *WASp* (C) pIIa-pIIb pairs at t20 in living pupae. DlGFP accumulated along the pIIa-pIIb interface in *Arp3* and *WASp* mutant cells (arrow; iRFF670nls, red, marked the pIIa and pIIb nuclei and loss of PH-ChFP; magenta marked the *Arp3* mutant cells). In contrast, DlGFP was not detected at this location in wild-type cells, presumably reflecting its rapid turnover (Trylinski et al., 2017).

(D–F′) DlGFP (anti-GFP, green) accumulated in the apical Spdo+ endosomes of pIIb (arrows; Spdo, magenta, and iRFF670nls, red, marked the pIIa and pIIb cells) (Couturier et al., 2014). Surface (D–F) and cross-section (D′, E′, and F′; apical, up) views are shown.

(G and H) Accumulation of DlGFP (green) in apical endosomes of pIIb (arrow; iRFF670nls, red) in living pupae. Surface (G) and cross-section (G′; apical, up) views are shown, along with the quantification of direct DlGFP fluorescence in apical endosomes (H). A significant decrease in the endosomal accumulation of DlGFP was measured upon the loss of *Arp3* and *WASp* activities (Kruskal-Wallis test, $p = 1.2 \times 10^{-3}$; Wilcoxon signed-rank test, ***$p < 0.001$; $n \geq 18$ cells, ≥ 2 pupae).

(I–K) Analysis of Dl endocytosis (endo-Dl, magenta) in fixed wild-type (I), *Arp3* (J; clones marked by the loss of PH-ChFP, magenta), and mutant *WASp* cells (K). DlgGFP (green) was used as a membrane marker. The pIIa-pIIb cells were marked by iRFP670nls (red). Snapshots of the corresponding dividing SOP cells are shown as insets.

(L–O) The number of endo-Dl+ endosomes (per pIIb cell; L and N) and the total intensity of these endo-Dl+ endosomes (per pIIb cell; M and O) are shown. The number of endosomes (L) and the level of endo-Dl (M) were both decreased in *Arp3* and *WASp* pIIb cells compared to wild-type pIIb at t5–t30 (L and M), but not in >t30 pIIb cells (N and O), indicating that Arp3 and WASp are required early but not late for the endocytosis of Dl. Kruskal-Wallis test, $p = 9.9 \times 10^{-5}$ (L) and $p = 1.9 \times 10^{-4}$ (M); ANOVA, $p = 0.2$ (N) and $p = 0.48$ (O); Wilcoxon signed-rank or Student's t test, ***$p < 0.001$; $n \geq 15$ cells, ≥ 3 pupae.

See also Figure S4.

apical endosomes where DlGFP colocalized with Sanpodo (Spdo) (Couturier et al., 2013; Hutterer and Knoblich, 2005; O'Connor-Giles and Skeath, 2003; Figures 4D–4F′) and found that the loss of Arp3 and WASp activities led to a strong loss of DlGFP accumulation in these apical endosomes at t20 (Figures 4G and 4H). These data therefore suggest that *Arp3* and *WASp* are required for the efficient endocytosis of Dl in pIIb.

To study the endocytosis of Dl during cytokinesis, when the activities of WASp and Arp2/3 are required for the production of NICD (Figures 1B and 2A), we combined an antibody uptake assay with live imaging (Figures 4I–4K and S4) and monitored the endocytosis of Dl during cytokinesis (from t5 to t30) and after cytokinesis (>t30). Analysis of Dl endocytosis during cytokinesis revealed a decrease in the number of Dl+ endosomes and in the

total amount of internalized Dl in *Arp3* and *WASp* mutant pIIb cells compared to wild-type controls (Figures 4L and 4M). Consistent with earlier findings (Rajan et al., 2009), the endocytosis of Dl was only decreased and not abolished in *Arp3* and *WASp* mutant cells. We therefore conclude that WASp-mediated activation of Arp2/3 promotes the efficient endocytosis of Dl during cytokinesis (<t30). In contrast, analysis of Dl endocytosis after cytokinesis (>t30) showed no significant difference between wild-type and mutant cells (Figures 4N and 4O). This revealed that the activities of WASp and Arp2/3 become dispensable for the endocytosis of Dl after cytokinesis. This finding is consistent with our observation that low NICD levels are produced in Arp3 and WASp mutant pIIa cells at t30–t60 (Figures 1B and 2A). We conclude that the activation of Arp2/3 by WASp is required for the efficient endocytosis of Dl only during a specific time window that corresponds to cytokinesis. We propose that Arp2/3 and WASp promote Notch receptor activation in pIIa by providing a strong pulling force associated with the endocytosis of Dl and that this extra force is needed only during cytokinesis.

DISCUSSION

Our study showed that Arp2/3 has two separable activities in asymmetric cell divisions: Arp2/3 promotes the rapid expansion of the new cell-cell contact and stimulates the endocytosis of Dl from this cell-cell contact to regulate intra-lineage fate decisions by Notch. These two activities involve distinct NPFs. SCAR, downstream of Rac, promotes the formation of a dense F-actin network around the midbody to generate a force that regulates cell-cell contact between sister cells and facilitates withdrawal of the membranes of the neighboring cells (Herszterg et al., 2013). SCAR, however, is largely dispensable for Notch receptor activation, suggesting that the force required for contact expansion is not key for Notch receptor activation. In contrast, WASp is required for Notch signaling but is dispensable for contact expansion during cytokinesis. While these two functions of Arp2/3 are separable, a functional interplay is possible, if not likely. For instance, Rac and SCAR may facilitate the activity of WASp in Dl endocytosis through the recruitment of Arp2/3 along the pIIa-pIIb interface.

Before the present study, WASp-mediated activation of Arp2/3 was thought to regulate the intracellular trafficking of internalized Dl, not its endocytosis (Rajan et al., 2009). This model assumed that Dl signals at the apical membrane, which seems unlikely since we recently showed that NICD originates from the lateral membrane during cytokinesis (Trylinski et al., 2017). Here, using a time-resolved endocytosis assay, we show that WASp-mediated activation of Arp2/3 is required to promote the endocytosis of Dl during cytokinesis, but not afterward. The specific time window during which the activities of WASp and Arp3 are required may explain why this requirement had previously been missed (Rajan et al., 2009). In analogy to the role of WASp in yeast (Mund et al., 2018; Picco et al., 2018), we propose that WASp is recruited at sites of Dl endocytosis to form a branched actin network that provides an inward pushing force onto the invaginated membrane. This would increase the efficiency of endocytosis—hence the rate of the force-dependent activation of Notch. Accordingly, WASp would play a modulatory role, which is critical within a defined time window. Consistent with this view, the

WASp mutant bristle phenotype can be suppressed by lowering the threshold for NICD levels in flies with reduced levels of the CSL co-repressor Hairless (Ben-Yaacov et al., 2001).

We wondered why WASp and Arp3 are required only during cytokinesis for the endocytosis of Dl. WASp is likely to have a general function in endocytosis in *Drosophila*, as in other organisms (Mund et al., 2018; Picco et al., 2018), and may therefore regulate the endocytosis of many cargoes, including Dl, throughout development (Georgiou et al., 2008; Leibfried et al., 2008). Consistent with a general function of WASp, it is ubiquitously expressed and is not specifically upregulated in sensory lineages (Rodriguez-Mesa et al., 2012). However, the role of WASp-activated Arp2/3 in endocytosis is essential, at the organismal level, only in the context of intra-lineage decisions regulated by Notch (Ben-Yaacov et al., 2001; Gohl et al., 2010; Legent et al., 2012). This specificity may be explained by when Notch signals, namely, at the end of mitosis. It is well established that clathrin-mediated endocytosis is shut down at mitosis and is progressively restored during cytokinesis (Fielding and Royle, 2013; Raucher and Sheetz, 1999). One mechanism contributing to this inhibition throughout mitosis is increased membrane tension (Fielding and Royle, 2013). Since an increased requirement for actin is observed in cells in which membrane tension is high (Kaur et al., 2014), we speculate that the endocytosis of Dl more critically depends upon actin regulation by WASp during cytokinesis due to increased membrane tension. In other words, we propose that the pushing force provided by WASp-induced F-actin is needed for the efficient endocytosis of Dl to counteract the increased membrane tension associated with mitosis. Thus, while WASp and Arp2/3 likely play a general role in endocytosis, their activities become critical for the mechanical activation of Notch only when the inhibition of endocytosis needs to be overcome in late mitosis.

The requirement of WASp for Notch receptor activation is symmetric to those of Epsin, a conserved endocytic adaptor that helps generate the force for membrane invagination during endocytosis (Messa et al., 2014). Epsin is generally required for ligand endocytosis and Notch signaling in flies (Wang and Struhl, 2004) and mammals (Chen et al., 2009; Meloty-Kapella et al., 2012), with the exception of Notch-mediated intra-lineage decisions, as revealed by the development of sensory bristles in *epsin* mutant clones (Wang and Struhl, 2004). We speculate that the inhibition of Epsin at mitosis, possibly via its phosphorylation by CDK1/Cdc2 (Chen et al., 1999; Kariya et al., 2000), renders necessary the extra pushing force provided by WASp for the efficient endocytosis of Dl.

In summary, we propose a model whereby the activity of WASp-Arp2/3 generally increases the efficiency of endocytosis and becomes specifically required only during cytokinesis, when Dl activates Notch to mediate intra-lineage decisions. This model may be general and apply to mammalian tissues where Notch is known to regulate intra-lineage decisions (Dong et al., 2012; Pardo-Saganta et al., 2015). N-WASp, the ubiquitously expressed WASp in mammals, is required for the maintenance of skin progenitor cells and hair follicle cycling in the mouse (Lyubimova et al., 2010), and Notch plays a critical role in the self-renewal of skin stem cells (Blanpain et al., 2006; Martincorena et al., 2015). Whether Notch signaling is regulated by N-WASp in this context remains to be examined.

STAR★METHODS

Detailed methods are provided in the online version of this paper and include the following:

- KEY RESOURCES TABLE
- LEAD CONTACT AND MATERIALS AVAILABILITY
- EXPERIMENTAL MODEL AND SUBJECT DETAILS
- METHOD DETAILS
  - Transgenes
  - Live-imaging and analysis of cell-cell contact
  - Immunostaining of staged pIIa-pIIb
  - Dl endocytosis assay
- QUANTIFICATION AND STATISTICAL ANALYSIS

AUTHOR CONTRIBUTIONS

M.T. performed all of the experiments and the data analysis. M.T. and F.S. designed the experiments and wrote the manuscript.

DECLARATION OF INTERESTS

The authors declare no competing interests.

REFERENCES

Aerts, S., Quan, X.J., Claeys, A., Naval Sanchez, M., Tate, P., Yan, J., and Hassan, B.A. (2010). Robust target gene discovery through transcriptome perturbations and genome-wide enhancer predictions in Drosophila uncovers a regulatory basis for sensory specification. PLoS Biol. *8*, e1000435.

Alekhina, O., Burstein, E., and Billadeau, D.D. (2017). Cellular functions of WASP family proteins at a glance. J. Cell Sci. *130*, 2235–2241.

Ben-Yaacov, S., Le Borgne, R., Abramson, I., Schweisguth, F., and Schejter, E.D. (2001). Wasp, the Drosophila Wiskott-Aldrich syndrome gene homologue, is required for cell fate decisions mediated by Notch signaling. J. Cell Biol. *152*, 1–13.

Blanpain, C., Lowry, W.E., Pasolli, H.A., and Fuchs, E. (2006). Canonical notch signaling functions as a commitment switch in the epidermal lineage. Genes Dev. *20*, 3022–3035.

Buszczak, M., Paterno, S., Lighthouse, D., Bachman, J., Planck, J., Owen, S., Skora, A.D., Nystul, T.G., Ohlstein, B., Allen, A., et al. (2007). The carnegie protein trap library: a versatile tool for Drosophila developmental studies. Genetics *175*, 1505–1531.

Campellone, K.G., and Welch, M.D. (2010). A nucleator arms race: cellular control of actin assembly. Nat. Rev. Mol. Cell Biol. *11*, 237–251.

Chen, H., Slepnev, V.I., Di Fiore, P.P., and De Camilli, P. (1999). The interaction of epsin and Eps15 with the clathrin adaptor AP-2 is inhibited by mitotic phosphorylation and enhanced by stimulation-dependent dephosphorylation in nerve terminals. J. Biol. Chem. *274*, 3257–3260.

Chen, H., Ko, G., Zatti, A., Di Giacomo, G., Liu, L., Raiteri, E., Perucco, E., Collesi, C., Min, W., Zeiss, C., et al. (2009). Embryonic arrest at midgestation and disruption of Notch signaling produced by the absence of both epsin 1 and epsin 2 in mice. Proc. Natl. Acad. Sci. USA *106*, 13838–13843.

Corson, F., Couturier, L., Rouault, H., Mazouni, K., and Schweisguth, F. (2017). Self-organized Notch dynamics generate stereotyped sensory organ patterns in *Drosophila*. Science *356*, eaai7407.

Cotton, M., Benhra, N., and Le Borgne, R. (2013). Numb inhibits the recycling of Sanpodo in Drosophila sensory organ precursor. Curr. Biol. *23*, 581–587.

Couturier, L., Vodovar, N., and Schweisguth, F. (2012). Endocytosis by Numb breaks Notch symmetry at cytokinesis. Nat. Cell Biol. *14*, 131–139.

Couturier, L., Mazouni, K., and Schweisguth, F. (2013). Numb localizes at endosomes and controls the endosomal sorting of notch after asymmetric division in Drosophila. Curr. Biol. *23*, 588–593.

Couturier, L., Trylinski, M., Mazouni, K., Darnet, L., and Schweisguth, F. (2014). A fluorescent tagging approach in Drosophila reveals late endosomal trafficking of Notch and Sanpodo. J. Cell Biol. *207*, 351–363.

de Chaumont, F., Dallongeville, S., Chenouard, N., Hervé, N., Pop, S., Provoost, T., Meas-Yedid, V., Pankajakshan, P., Lecomte, T., Le Montagner, Y., et al. (2012). Icy: an open bioimage informatics platform for extended reproducible research. Nat. Methods *9*, 690–696.

Del Signore, S.J., Cilla, R., and Hatini, V. (2018). The WAVE Regulatory Complex and Branched F-Actin Counterbalance Contractile Force to Control Cell Shape and Packing in the Drosophila Eye. Dev. Cell *44*, 471–483.e4.

Dong, Z., Yang, N., Yeo, S.-Y., Chitnis, A., and Guo, S. (2012). Intralineage directional Notch signaling regulates self-renewal and differentiation of asymmetrically dividing radial glia. Neuron *74*, 65–78.

Eden, S., Rohatgi, R., Podtelejnikov, A.V., Mann, M., and Kirschner, M.W. (2002). Mechanism of regulation of WAVE1-induced actin nucleation by Rac1 and Nck. Nature *418*, 790–793.

Fielding, A.B., and Royle, S.J. (2013). Mitotic inhibition of clathrin-mediated endocytosis. Cell. Mol. Life Sci. *70*, 3423–3433.

Georgiou, M., Marinari, E., Burden, J., and Baum, B. (2008). Cdc42, Par6, and aPKC regulate Arp2/3-mediated endocytosis to control local adherens junction stability. Curr. Biol. *18*, 1631–1638.

Gho, M., Bellaïche, Y., and Schweisguth, F. (1999). Revisiting the Drosophila microchaete lineage: a novel intrinsically asymmetric cell division generates a glial cell. Development *126*, 3573–3584.

Gohl, C., Banovic, D., Grevelhörster, A., and Bogdan, S. (2010). WAVE forms hetero- and homo-oligomeric complexes at integrin junctions in Drosophila visualized by bimolecular fluorescence complementation. J. Biol. Chem. *285*, 40171–40179.

Goley, E.D., and Welch, M.D. (2006). The ARP2/3 complex: an actin nucleator comes of age. Nat. Rev. Mol. Cell Biol. *7*, 713–726.

Gomes, J.E., Corado, M., and Schweisguth, F. (2009). Van Gogh and Frizzled act redundantly in the Drosophila sensory organ precursor cell to orient its asymmetric division. PLoS One *4*, e4485.

Guisoni, N., Martinez-Corral, R., Garcia-Ojalvo, J., and de Navascués, J. (2017). Diversity of fate outcomes in cell pairs under lateral inhibition. Development *144*, 1177–1186.

Hakeda-Suzuki, S., Ng, J., Tzu, J., Dietzl, G., Sun, Y., Harms, M., Nardine, T., Luo, L., and Dickson, B.J. (2002). Rac function and regulation during Drosophila development. Nature *416*, 438–442.

Henrique, D., and Schweisguth, F. (2019). Mechanisms of Notch signaling: a simple logic deployed in time and space. Development *146*, dev172148.

Herszterg, S., Leibfried, A., Bosveld, F., Martin, C., and Bellaiche, Y. (2013). Interplay between the dividing cell and its neighbors regulates adherens junction formation during cytokinesis in epithelial tissue. Dev. Cell *24*, 256–270.

Hutterer, A., and Knoblich, J.A. (2005). Numb and alpha-Adaptin regulate Sanpodo endocytosis to specify cell fate in Drosophila external sensory organs. EMBO Rep. *6*, 836–842.

Johnson, S.A., Zitserman, D., and Roegiers, F. (2016). Numb regulates the balance between Notch recycling and late-endosome targeting in Drosophila neural progenitor cells. Mol. Biol. Cell *27*, 2857–2866.

Kaksonen, M., and Roux, A. (2018). Mechanisms of clathrin-mediated endocytosis. Nat. Rev. Mol. Cell Biol. *19*, 313–326.

Kariya, K., Koyama, S., Nakashima, S., Oshiro, T., Morinaka, K., and Kikuchi, A. (2000). Regulation of complex formation of POB1/epsin/adaptor protein complex 2 by mitotic phosphorylation. J. Biol. Chem. *275*, 18399–18406.

Kaur, S., Fielding, A.B., Gassner, G., Carter, N.J., and Royle, S.J. (2014). An unmet actin requirement explains the mitotic inhibition of clathrin-mediated endocytosis. eLife *3*, e00829.

Kim, A.S., Kakalis, L.T., Abdul-Manan, N., Liu, G.A., and Rosen, M.K. (2000). Autoinhibition and activation mechanisms of the Wiskott-Aldrich syndrome protein. Nature *404*, 151–158.

Kopan, R., and Ilagan, M.X. (2009). The canonical Notch signaling pathway: unfolding the activation mechanism. Cell *137*, 216–233.

Langridge, P.D., and Struhl, G. (2017). Epsin-Dependent Ligand Endocytosis Activates Notch by Force. Cell *171*, 1383–1396.e12.

Le Borgne, R., and Schweisguth, F. (2003). Unequal segregation of Neuralized biases Notch activation during asymmetric cell division. Dev. Cell *5*, 139–148.

Legent, K., Steinhauer, J., Richard, M., and Treisman, J.E. (2012). A screen for X-linked mutations affecting Drosophila photoreceptor differentiation identifies Casein kinase 1α as an essential negative regulator of wingless signaling. Genetics *190*, 601–616.

Leibfried, A., Fricke, R., Morgan, M.J., Bogdan, S., and Bellaiche, Y. (2008). Drosophila Cip4 and WASp define a branch of the Cdc42-Par6-aPKC pathway regulating E-cadherin endocytosis. Curr. Biol. *18*, 1639–1648.

Lovendahl, K.N., Blacklow, S.C., and Gordon, W.R. (2018). The Molecular Mechanism of Notch Activation. In Molecular Mechanisms of Notch Signaling, T. Borggrefe and B.D. Giaimo, eds. (Springer), pp. 47–58.

Lyubimova, A., Garber, J.J., Upadhyay, G., Sharov, A., Anastasoaie, F., Yajnik, V., Cotsarelis, G., Dotto, G.P., Botchkarev, V., and Snapper, S.B. (2010). Neural Wiskott-Aldrich syndrome protein modulates Wnt signaling and is required for hair follicle cycling in mice. J. Clin. Invest. *120*, 446–456.

Martincorena, I., Roshan, A., Gerstung, M., Ellis, P., Van Loo, P., McLaren, S., Wedge, D.C., Fullam, A., Alexandrov, L.B., Tubio, J.M., et al. (2015). Tumor evolution. High burden and pervasive positive selection of somatic mutations in normal human skin. Science *348*, 880–886.

Meloty-Kapella, L., Shergill, B., Kuon, J., Botvinick, E., and Weinmaster, G. (2012). Notch ligand endocytosis generates mechanical pulling force dependent on dynamin, epsins, and actin. Dev. Cell *22*, 1299–1312.

Messa, M., Fernández-Busnadiego, R., Sun, E.W., Chen, H., Czapla, H., Wrasman, K., Wu, Y., Ko, G., Ross, T., Wendland, B., and De Camilli, P. (2014). Epsin deficiency impairs endocytosis by stalling the actin-dependent invagination of endocytic clathrin-coated pits. eLife *3*, e03311.

Mullins, R.D., and Pollard, T.D. (1999). Rho-family GTPases require the Arp2/3 complex to stimulate actin polymerization in Acanthamoeba extracts. Curr. Biol. *9*, 405–415.

Mund, M., van der Beek, J.A., Deschamps, J., Dmitrieff, S., Hoess, P., Monster, J.L., Picco, A., Nédélec, F., Kaksonen, M., and Ries, J. (2018). Systematic Nanoscale Analysis of Endocytosis Links Efficient Vesicle Formation to Patterned Actin Nucleation. Cell *174*, 884–896.e17.

Nagel, B.M., Bechtold, M., Rodriguez, L.G., and Bogdan, S. (2017). Drosophila WASH is required for integrin-mediated cell adhesion, cell motility and lysosomal neutralization. J. Cell Sci. *130*, 344–359.

O'Connor-Giles, K.M., and Skeath, J.B. (2003). Numb inhibits membrane localization of Sanpodo, a four-pass transmembrane protein, to promote asymmetric divisions in Drosophila. Dev. Cell *5*, 231–243.

Pardo-Saganta, A., Tata, P.R., Law, B.M., Saez, B., Chow, R.D.-W., Prabhu, M., Gridley, T., and Rajagopal, J. (2015). Parent stem cells can serve as niches for their daughter cells. Nature *523*, 597–601.

Picco, A., Kukulski, W., Manenschijn, H.E., Specht, T., Briggs, J.A.G., and Kaksonen, M. (2018). The contributions of the actin machinery to endocytic membrane bending and vesicle formation. Mol. Biol. Cell *29*, 1346–1358.

Pollard, T.D. (2007). Regulation of actin filament assembly by Arp2/3 complex and formins. Annu. Rev. Biophys. Biomol. Struct. *36*, 451–477.

Pollard, T.D., and Borisy, G.G. (2003). Cellular motility driven by assembly and disassembly of actin filaments. Cell *112*, 453–465.

Rajan, A., Tien, A.-C., Haueter, C.M., Schulze, K.L., and Bellen, H.J. (2009). The Arp2/3 complex and WASp are required for apical trafficking of Delta into microvilli during cell fate specification of sensory organ precursors. Nat. Cell Biol. *11*, 815–824.

Raucher, D., and Sheetz, M.P. (1999). Membrane expansion increases endocytosis rate during mitosis. J. Cell Biol. *144*, 497–506.

Rauzi, M., Lenne, P.-F., and Lecuit, T. (2010). Planar polarized actomyosin contractile flows control epithelial junction remodelling. Nature *468*, 1110–1114.

Rhyu, M.S., Jan, L.Y., and Jan, Y.N. (1994). Asymmetric distribution of numb protein during division of the sensory organ precursor cell confers distinct fates to daughter cells. Cell *76*, 477–491.

Rodriguez-Mesa, E., Abreu-Blanco, M.T., Rosales-Nieves, A.E., and Parkhurst, S.M. (2012). Developmental expression of Drosophila Wiskott-Aldrich Syndrome family proteins. Dev. Dyn. *241*, 608–626.

Rohatgi, R., Ma, L., Miki, H., Lopez, M., Kirchhausen, T., Takenawa, T., and Kirschner, M.W. (1999). The interaction between N-WASP and the Arp2/3 complex links Cdc42-dependent signals to actin assembly. Cell *97*, 221–231.

Rotty, J.D., Wu, C., and Bear, J.E. (2013). New insights into the regulation and cellular functions of the ARP2/3 complex. Nat. Rev. Mol. Cell Biol. *14*, 7–12.

Schweisguth, F. (2015). Asymmetric cell division in the Drosophila bristle lineage: from the polarization of sensory organ precursor cells to Notch-mediated binary fate decision. Wiley Interdiscip. Rev. Dev. Biol. *4*, 299–309.

Shaya, O., Binshtok, U., Hersch, M., Rivkin, D., Weinreb, S., Amir-Zilberstein, L., Khamaisi, B., Oppenheim, O., Desai, R.A., Goodyear, R.J., et al. (2017). Cell-Cell Contact Area Affects Notch Signaling and Notch-Dependent Patterning. Dev. Cell *40*, 505–511.e6.

Shcherbakova, D.M., and Verkhusha, V.V. (2013). Near-infrared fluorescent proteins for multicolor in vivo imaging. Nat. Methods *10*, 751–754.

Tal, T., Vaizel-Ohayon, D., and Schejter, E.D. (2002). Conserved interactions with cytoskeletal but not signaling elements are an essential aspect of Drosophila WASp function. Dev. Biol. *243*, 260–271.

Trylinski, M., Mazouni, K., and Schweisguth, F. (2017). Intra-lineage Fate Decisions Involve Activation of Notch Receptors Basal to the Midbody in Drosophila Sensory Organ Precursor Cells. Curr. Biol. *27*, 2239–2247.e3.

Verboon, J.M., Decker, J.R., Nakamura, M., and Parkhurst, S.M. (2018). Wash exhibits context-dependent phenotypes and, along with the WASH regulatory complex, regulates Drosophila oogenesis. J. Cell Sci. *131*, jcs211573.

Wang, W., and Struhl, G. (2004). Drosophila Epsin mediates a select endocytic pathway that DSL ligands must enter to activate Notch. Development *131*, 5367–5380.

Yamada, S., and Nelson, W.J. (2007). Localized zones of Rho and Rac activities drive initiation and expansion of epithelial cell-cell adhesion. J. Cell Biol. *178*, 517–527.

Zallen, J.A., Cohen, Y., Hudson, A.M., Cooley, L., Wieschaus, E., and Schejter, E.D. (2002). SCAR is a primary regulator of Arp2/3-dependent morphological events in Drosophila. J. Cell Biol. *156*, 689–701.

STAR★METHODS

KEY RESOURCES TABLE

REAGENT or RESOURCE	SOURCE	IDENTIFIER
Antibodies		
Mouse monoclonal anti-Delta-ECD (concentrate)	Developmental Studies Hybridoma Bank	DSHB C594.9B; RRID:AB_528194
Goat polyclonal anti-GFP	Abcam	Ab6673; RRID:AB_305643
Guinea-pig polyclonal anti-Sanpodo	Gift from J.Knoblich	RRID:AB_2568071
Experimental Models: Organisms/Strains		
D.melanogaster: NiGFP CRISPR knock-in: Ni^{GFP}	Trylinski et al., 2017	N/A
D.melanogaster: DlGFP CRISPR knock-in: w;; Dl^{GFP}	Corson et al., 2017	Flybase: FBal0344893
D.melanogaster: SOP nuclear marker, transgenic lines: w neur-iRFP670nls and w; neur-iRFP670nls	Couturier et al., 2014	Flybase: FBtp0097597
D.melanogaster: SOP membrane marker, transgenic line: w; neur-PH-iRFP670	This study	N/A
D.melanogaster: SOP-specific expression of Gal80, transgenic line: w;; neur-Gal80	This study	N/A
D.melanogaster: Arp3 mutant allele (premature stop codon at amino-acid position 378): w;; $Arp3^{515FC}$ FRT80B/ TM3, P{GAL4-Kr.C}DC2, P{UAS-GFP.S65T}DC10, Sb1	Rajan et al., 2009	Bloomington: BDSC39727 Flybase: FBal0269076
D.melanogaster: WASp mutant allele (truncated protein lacking the WCA domain): w;; $WASp^3$ FRT82B/TM6B Tb	Ben Yaacov et al., 2001	Bloomington: BDSC39725 Flybase: FBal0121873
Recombinant DNA		
Plasmid: pStinger-attB-neurGal80	This study	N/A
Plasmid: pStinger-attB-neurPH-iRFP670	This study	N/A
Software and Algorithms		
Icy	de Chaumont et al., 2012	http://icy.bioimageanalysis.org/

LEAD CONTACT AND MATERIALS AVAILABILITY

Further information and requests for resources and reagents should be directed to and will be fulfilled by the Lead Contact, François Schweisguth (fschweis@pasteur.fr).

EXPERIMENTAL MODEL AND SUBJECT DETAILS

aThe following lines were used in this study: Ni^{GFP}, a GFP knock-in line (Trylinski et al., 2017), Dl^{GFP}, a GFP knock-in line (Corson et al., 2017), $Arp3^{515FC}$ (BL-39727), $WASp^3$ (BL-39725), *Df(3R)Exel6210* (BL-7688), *Dlg-GFP* (BL-50859), $SCAR^{Δ37}$ (BL-8754), $Rac1^{J11}$ $Rac2^Δ$ FRT2A $Mtl^Δ$ (BL-6678), UAS-$Rac1^{N17}$ (BL-6292), *Resille-GFP* (also known as CG8668-GFP) (Buszczak et al., 2007), UAS-mCherry-CAAX (BL-59021), ubi-PLCγPH-ChFP (Herszterg et al., 2013), UASp-Utrn-GFP (Rauzi et al., 2010), LifeAct-GFP (BL-35554), LifeAct-Ruby (BL-35545), Arp3-GFP (BL-39722), Rac1GFP (BL-52285), Cherry-MyoII (BL-59024), neur-H2B-RFP (Gomes et al., 2009), neur-iRFP670nls (Couturier et al., 2014), neur-PH-iRFP670 (PH domain of PLC-γ fused to iRFP670 under the control of the *neur* regulatory sequences; this study), neur-Gal80 (Gal80 under the control of the *neur* regulatory sequences; this study), *Ubx-flp*, $neur^{PGal4}$ (Gho et al., 1999), *pnr-Gal4* (BL-3039), tub-Gal80^{ts} (BL-7018 and −7019).

Somatic clones were generated using the FLP/FRT system using *Ubx-flp* combined with *FRT40A* ($SCAR^{Δ37}$ mutant clones), *FRT80B* ($Arp3^{515FC}$ mutant clones) and *FRT2A* (*rac* mutant clones). *WASp* mutant pupae were $WASp^3$/*Df(3R)6210* (deficient background).

To express mCherry-CAAX specifically in epidermal cells of the notum, we combined activation in all cells using *pnr-Gal4* with inhibition of this activation in SOPs using *neur-Gal80*. Additionally, to prevent early expression of mCherry-CAAX, i.e., prior to SOP selection, the activity of Gal4 was temporally restricted using tub-Gal80^{ts}. Larvae and early pupae were grown at 18°C and

shifted at 29°C just prior to head eversion (17h h APF at 18°C), at the stage when SOPs become specified (Corson et al., 2017). This strategy allowed for the expression of mCherry-CAAX for ~6 h before SOPs divide.

To avoid embryonic lethality, the expression of $Rac1^{DN}$ by $neur^{PGal4}$ was rendered conditional using $tub\text{-}Gal80^{ts}$. Larvae were grown at 18°C and shifted at 29°C at 0 h APF. Dividing SOPs were imaged at 14 h APF.

METHOD DETAILS

Transgenes
The following transgenes were produced:

- neur-PH-iRFP670: the codon-optimized sequence of the *iRFP670* gene (Shcherbakova and Verkhusha, 2013) was PCR-amplified from neur-nlsFP670 (Couturier et al., 2014), fused to the PH domain of the human *PLC-γ* gene using overlapping PCR synthesis and cloned into the Stinger-attB-p*neur*-GFP plasmid (Aerts et al., 2010) where it replaced GFP. After sequencing, the resulting transgene was inserted at position 28E7 (PB[y⁺ attP-3B]VK02).
- neur-Gal80: the sequence of the *Gal80* gene was PCR-amplified from pCaspeR4-Gal80 and inserted into the Stinger-attB-*neur*-GFP plasmid (Aerts et al., 2010) where it replaced GFP. After sequencing, the resulting transgene was inserted at position 99F8 (PB[y⁺ attP-9A]VK20).

Integrations were mediated by phiC31. BAC injections were performed by BestGene, Inc.

Live-imaging and analysis of cell-cell contact
Staged pupae were prepared for live-imaging as described earlier (Couturier et al., 2014). Live-imaging was performed at 20 ± 2°C with a scanning confocal microscope (LSM780, Zeiss) with a 63x Plan APO N.A. 1.4 DIC M27 objective. Images were acquired using z stacks (Δz = 0.5μm) in time-series.

Notch activity dynamics were determined by measuring the GFP fluorescence produced by NiGFP in pIIa and pIIb nuclei, as described earlier (Trylinski et al., 2017). To prevent photobleaching, each pIIa-pIIb pair was imaged at a single time point (12-20 values were acquired per pupa). For each pupa, the raw data were normalized by the mean value of nuclear NiGFP in pIIa and pIIb at t10.

The LifeAct-GFP and Utrn-GFP signals were quantified on 2-image projections (Δz = 1μm) corresponding to the region just below the midbody. Intensity profiles were obtained using a manually defined ROI spanning the pIIa-pIIb interface. Images of the same pIIa-pIIb pairs were acquired at t10, t20 and t30.

Lateral surfaces were quantified in SOPs surrounded by epidermal cells expressing a membrane marker. First, the membranes of the neighboring epidermal cells which locate between pIIa and pIIb were segmented automatically in each z section using the PH-ChFP, mCherry-CAAX or Resille-GFP markers. The lateral interface was next semi-automatically and independently segmented using the DlgGFP, PH-iRFP670 or PH-ChFP markers. Segmented interfaces were subsequently processed using the "3D ImageJ Suite" on Fiji to reconstruct a 3D object and determine its surface area. Images of the same pIIa-pIIb pairs were acquired at t10, t20, t30 and t60. In $Rac1^{DN}$ cells, edges of interfaces were determined using the weak actin patches detected at lateral tricellular junctions. Contact width corresponds here to the distance between these two vertices.

Movies were acquired with a 1-minute (movie 1) or a 10 s frame rate (movies 2-4) and a Δz = 0.5μm step. Images were furthered filtered with a Gaussian blur (σ = 1) for presentation.

Immunostaining of staged pIIa-pIIb
Staged pupae expressing DlGFP were mounted for live imaging and SOPs dividing within a 20 min time window (t0-t20) were selected. After an additional 5 min, these pupae were dissected and fixed. This dissection step took ~5 minutes, so that pIIa-pIIb pairs were t10-t30. Nota were then processed for antibody staining using goat anti-GFP (1:1000, Abcam) and guinea-pig anti-Spdo (1:1000, gift from J. Knoblich) to mark the pIIb subapical endosomes. Secondary antibodies (1:1000) were from Jackson ImmunoResearch Laboratories. DlGFP apical endosomes were automatically detected for quantification using the Spot Detector plugin under Icy (de Chaumont et al., 2012).

Dl endocytosis assay
SOPs undergoing the metaphase-anaphase transition were first selected in living pupae within a 10-min window to stay in the timing of cytokinesis (t0-t10). After this live imaging step, pupae were dissected and processed for antibody uptake (Couturier et al., 2014). This dissection step took ~5 min; hence pIIa-pIIb cells were t5-t15. Dissected and living nota were incubated 15 min with the anti-Dl antibody (mouse, 594.9B concentrate, 1:10, DHSB) in Schneider medium at 25°C (pIIa-pIIb cells were t20-t30), then fixed (paraformaldehyde 4%). Nota were then immunostained using goat anti-GFP (1:1000, Abcam) to detect Dlg-GFP. Secondary antibodies (1:1000) were from Jackson ImmunoResearch Laboratories.

Two categories of SOPs were studied. First, those that had divided during the 10 min of live imaging produced the t20-t30 pIIa-pIIb pairs. In these cells, endocytosis took place between t5 and t30. Second, SOPs that had divided prior to live imaging were used to study endocytosis after t30. These two categories of pIIa-pIIb pairs were identified by confocal microscopy on fixed nota based on

their position in the tissue and relative to the clone borders. Dl-positive vesicles were automatically detected for quantification using the Spot Detector plugin under Icy (de Chaumont et al., 2012).

QUANTIFICATION AND STATISTICAL ANALYSIS

The number of cells and pupae, p values and dispersion values (standard error of the mean, s.e.m.) are given in the figures and figure legends. The boxplots presented in Figure 4 are Tukey style, with outliers shown as empty black circles. Normal distribution was tested using the Shapiro-Wilk test. Statistical significance was first tested by Kruskall-Wallis or ANOVA tests, then by Wilcoxon signed-rank or Student's t tests.